Understanding changes in the Arctic basin sea ice mass budget as simulated by CCSM4: Implications from melt season characteristics and the surface albedo feedback

Daniel A. Pollak
SOARS® Summer 2010
Science Research Mentors:
Marika Holland, David Bailey, Alexandra Jahn
Writing and Communications Mentor:
Cindy Worster

Abstract Observations reveal alarming drops in Arctic sea ice extent, and climate models project that further changes will occur that could have global repercussions. An important aspect of this change is the surface albedo feedback, driven by the contrast between the albedos of snow/ice and the open ocean. This feedback causes ice to melt and overall albedos to decrease, amplifying surface warming in the Arctic. NCAR's newly released, fully coupled Community Climate System Model Version 4 (CCSM4) is used to assess long-term changes in the Arctic sea ice mass budget. Analysis of monthly-averaged mass budget time series from the 20th and 21st centuries revealed drastic changes from 1980-2050, the focus years of this study. While numerous factors determine the Arctic sea ice mass budget, we focus on the surface melt terms as they are most closely related to the surface albedo feedback. During the study period, annually averaged difference plots of sea ice thickness and area both revealed substantial decreases across the entire Arctic domain. Helping to clarify these long-term changes, new daily output data from the CCSM4 allowed for the examination of melt season characteristics such as onset and cessation dates as well as season duration. One of the most interesting aspects was the shift to earlier onset dates throughout the Arctic Basin. This shift, coupled with the seasonal solar cycle has substantial implications. Earlier onset dates imply an earlier decrease of albedo that overlaps with the seasonal maximum of downward shortwave radiation. This leads to increases in shortwave absorption and results in amplified ice melt, subsequently intensifying the surface albedo feedback. The strong relationship between earlier melt onset dates and increased absorbed radiation does exist and therefore is a key factor leading toward Arctic amplification.

Acknowledgements The Significant Opportunities in Atmospheric Research and Science (SOARS) Program is managed by the University Corporation for Atmospheric Research (UCAR) with support from participating universities. SOARS is funded by the National Science Foundation, the National Oceanic and Atmospheric Administration (NOAA) Climate Program Office, the NOAA Oceans and Human Health Initiative, the Center for Multi-Scale Modeling of Atmospheric Processes at Colorado State University, and the Cooperative Institute for Research in Environmental Sciences. SOARS is a partner project with Research Experience in Solid Earth Science for Student (RESESS).

1 Introduction

With the global human population nearing 7 billion, it is impossible to ignore the effect that human activity has on planet Earth. Burning of fossil fuels for transportation, agriculture, and industry has caused anthropogenic increases in greenhouse gas concentrations. In moderate amounts, these greenhouse gases act as a protective shield for the Earth. However, large concentrations of these gases can act as a stronger insulator leading to warming conditions at the Earth's surface. Concentrations of carbon dioxide (CO^2), a key greenhouse gas, have increased by 15% during the last thirty years to 390 parts per million (ppm). These increases are related to the warming of globally averaged temperatures (figure 1), with many recent years labeled the warmest since records began in the 1880s. Notably, the 20 warmest years (since 1880) have occurred after 1981 and the 10 warmest have occurred in the last 12 years (Menne and Kennedy 2008). In particular, the poles are heavily susceptible to an increased

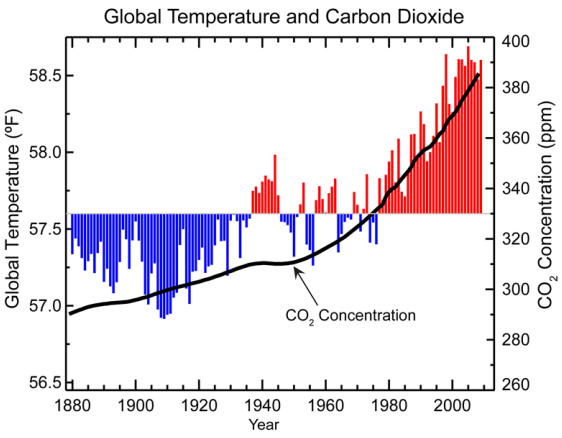

Figure 1 Annually averaged global temperatures and CO_2 concentrations from when records began in 1880 to the present. Red (blue) columns indicate temperatures that are above (below) the long term average. A trend between increasing CO_2 and warmer temperatures is evident.

greenhouse gas signal. A consensus of models predict an increase of Arctic basin temperatures by 2 to 3 times the comprehensive global trend by the year 2100 (Holland 2010). Rapid warming of Arctic temperatures, termed Arctic amplification, can have drastic consequences on the global climate system due to the delicate, yet intricate nature of sea ice, oceanic, atmospheric, and landmass interactions.

Given that Arctic sea ice covers up to 3% of the Earth's surface, Arctic amplification can be further attributed to changing perennial trends of this sea ice (Holland 2010). While seemingly insubstantial, this 3% partition contributes significantly to the climate system of the Arctic and the Earth as a whole. Variations and loss of sea ice have the potential to drive further changes in the atmosphere and ocean, influencing the surface energy budget as well as changes within the global hydrological cycle. Effects will be felt both locally and globally.

1.1 Arctic Sea Ice and Observations of Change:

The Arctic Ocean basin, located in the high latitudes of the Northern Hemisphere between continental North America and Eurasia, is visibly characterized by its sea ice. The sea ice, which is frozen ocean, waxes and wanes seasonally based on amounts of incoming solar radiation (insolation). Figure 21, shown later, provides a time series of average monthly insolation values for a particular point in the Beaufort Sea. The peak influx of insolation occurs during the summer in June when there are 24 hours of sunshine, while the near zero values for November, December, January, and February are indicative of the region's completely dark winters. Given the thermal lag time of the ocean, sea ice coverage reaches its' maximum extent during the month of March (at the end of the dark season) and its minima in ice extent in September, at the end of the summer. This seasonal process of changing sea ice extent is natural, but has recently seen perturbations toward a smaller ice pack, especially during the seasonal minimum in September. The maps of satellite observed sea ice extent in figure 2, compiled by the National Snow and Ice Data Center (NSIDC) provide a visual representation of the seasonal cycle as well as the decreasing trend in sea ice extent realized in the last 30 years. The seasonality is indicated by the larger sea ice coverage seen in March versus September. The

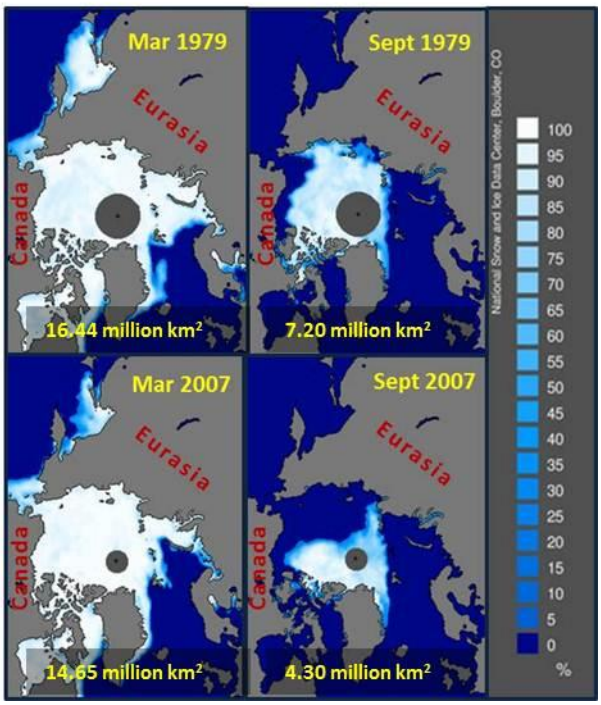

Figure 2 Observed monthly ice concentrations as seen by satellites. The seasonal cycle of waxing and waning ice is seen when comparing March and September. Beyond this cycle, a pronounced downward trend is seen between 1979 and 2007 (NSIDC).

distinct downward trend of sea ice from anthropogenic greenhouse gas sources is captured through the comparison between the 1979 and 2007 panels. The sea ice in March of both 1979 and 2007 cover the entire basin from the Canadian Arctic Archipelago to the coast of Eurasia. The decrease in ice between the two years clearly visible when comparing the September ice extents from 1979 to 2007. The trend seen in figure 2 was created through a composite of relatively recent satellite data, discussed below. To further understand implications of this downward trend, we used the CCSM4. But first is a discussion of the background of our current observational platform.

Satellites designed for the remote sensing of sea ice began operation in 1979 and are instrumental in visualizing and confirming the alarming decrease in sea ice realized since that time and into the present. The 29 year spread from 1979-2007 alone saw a 30% reduction in annually averaged sea ice extent (Holland et al. 2008). Initiation of NASA's Scanning Sensor Microwave Radiometer (SSMR) in 1979 provided the first reliable and comprehensive (and temporally consistent) look at sea ice. Previously, there were upward looking sonar data from submarines in the 1950s. However, these data were spatially and temporally sparse and could only be used to note general trends, not detailed analysis. Generally, soundings from 1958 to 1976 revealed an average ice thickness of 3.1 meters (m) which decreased to 1.8 m from the 1990s soundings. As the SSMR passed its life expectancy, a series of DMSP (Defense Meteorological Satellites Program- US Air Force) Special Sensor Microwave/Imager (SSM/I) were deployed to continue the time series (in 1987). Technological improvements through the turn of the 21st century have led to launches of higher caliber and functionality satellites, which provide data giving a look at sea ice change.

In these satellite images, sea ice extent is defined as a pixel where there is at least 15% fractional coverage of ice (Serreze et al. 2007). While all months have seen retreating ice, September has been the most dramatic with a downward trend of -10.7% per decade (figures 2 and 3). From 1979 to 2002 the negative trend was linear but recent years have shown acceleration in retreat. The perennial minima in September 2007 proved to be substantially anomalous with a season minimum ice extent of 4.3 million km^2. This represents a 23% reduction from the previous record minimum in September 2005 and a 3 standard deviation departure from the negative linear trend (Bitz and Lipscomb 1999, Holland 2010, Holland et al. 2008). While September 2008 (-16%) & 2009 saw ice extent minimums above the 2007 level, they still remained well below the previous 2005 record (Bitz and Lipscomb 1999). Despite these increases, the overall trend is uncontestably downward. Expected, year to year variations exist and are representative of intrinsic, or natural, variability of the climate system. Given the short record of these observations, it is of critical importance to simulate these recent changes through climate models so that we can help predict and understand determinants behind future changes. As mentioned above, we utilize NCAR's newly released Community Climate System Model Version 4. First, influential feedbacks thought to be important to the Arctic sea ice mass budget will be discussed.

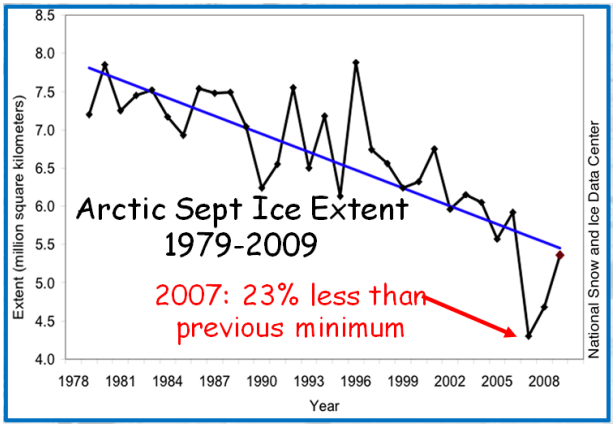

Figure 1 Satellite observations of September sea ice extent. While the overall trend is uncontestably downward, there are year to year variations, evident in the steep increase in 2008 and 2009 seen following the record minimum in 2007. In recent years, the downward trend has largely deviated from a linear decrease.

1.2 Surface mass budgets – surface albedo feedback

A climate feedback is defined as a process in the climate system that can either amplify or dampen in response to external forcings, such as increases in greenhouse gas concentrations. Sensitivity to these feedbacks, termed climate sensitivity, is largely a function of other feedbacks, in particular, radiative feedbacks. Radiative feedbacks involve solar shortwave and terrestrial longwave radiation fluxes that are highly influential on the climate system. They are often examined through associations with water vapor, clouds, snow and sea ice (Bony et al 2006). While there is growing evidence that indicates the increasing role polar cloud feedbacks play in Arctic amplification and climate sensitivity (Holland and Bitz, 2003; Vavrus 2004), we herein focus on the ice-snow albedo feedback, also known as a major contributor to Arctic amplification. This amplification, which was introduced by Manabe and Stouffer (1980) is a nearly unanimous feature of climate model simulations (Holland and Bitz 2003). A consensus of models from the Intergovernmental Panel on Climate Change Assessment Report 4 display a 2-3x larger surface temperature increase in the Arctic when compared to the average global temperature increase by 2100 (figure 4). Rind et al. (1995) showed that 20-40% of simulated temperature increases resulting from doubled CO2 concentrations (2xCO2) was a result of the changing sea ice cover.

Sea ice loss has implications in both the surface energy budget as well as the global hydrological cycle. These hydrological changes can come in the form of freshwater discharge, a result from melting ice. This subsequently decreases ocean salinity and can lead to large scale changes in ocean currents and the thermohaline circulation. Holland et al (Holland et al. 2007) predict an acceleration of the overall Arctic hydrological cycle driven by the freshening of the Arctic Ocean. Additionally, freshwater advections into the North Atlantic could have impacts to the global climate (Serreze et al. 2009).

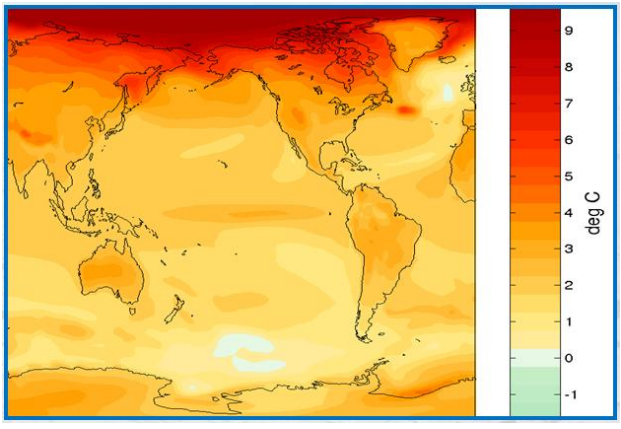

Figure 4 A composite of all models in the IPCC AR4 displaying surface temperature changes between 2005 and 2100. Arctic amplification is clearly visible by the dark reds.

More critical to this study and the realized downward trend in sea ice is the surface energy budget. This budget involves interactions between the ice, ocean and atmosphere, but for the scope of this project, we focus on the ice-atmosphere interface. As discussed above, the radiation fluxes are highly important in understanding sea ice changes, and are themselves a feedback, termed the surface albedo feedback.

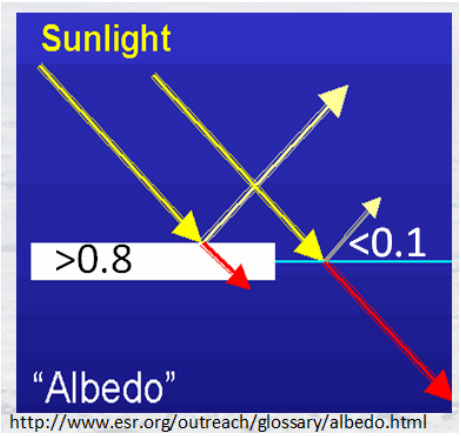

Figure 5 Concept driving the surface albedo feedback. Snow and ice have a high albedo of greater than 0.8, and open ocean - 0.1.

When incoming solar radiation (yellow arrows in figure 5), approach the Earth's surface, they are either reflected (white arrow) or absorbed (red arrow). The proportions between each are dependent on surface characteristics. Clean snow and ice reflect upwards of 80% of incoming solar radiation, absorbing less than 20%. Opposite, high latitude open ocean absorbs 90% of insolation reflecting a mere 10%. The representative term used to describe the reflected

radiation quantities is coined albedo and is unit-less, measured as a fraction of 1. For example, snow and ice have an albedo of 0.8+ (reflecting 80%+) while open ocean have albedos of 0.1 (figure 5).

Given the profound albedo spread between the two surfaces, increasing open ocean and decreasing sea ice is a striking and fundamental factor driving the surface albedo feedback. The sea ice also acts as an effective insulator between the ocean and atmosphere preventing the rapid transfer of heat and moisture between the two fluids. When sea ice extent decreases and larger cracks develop, additional open ocean is exposed, leading to increased shortwave absorption by the ocean. The direct atmosphere-ocean interface created allows for the direct transfer of heat and moisture and invokes further changes onto the system. Through this surface albedo feedback, it is possible to exacerbate perennial sea ice loss and Arctic amplification. As a result, analysis and understanding of changes in the ice mass budget is a critical point of interest in order to ascertain probable future conditions both locally and globally.

Figure 6 provides a summary of the surface albedo feedback. When surface albedo's decrease, more incoming solar radiation is absorbed by the ocean, land, and sea ice surfaces. This increases temperatures which subsequently melts more snow and sea ice. As a result, many variables in sea ice state change such as ice thickness, ice extent, and also the development of melt ponds which sit on the sea ice surface and have lower albedos (0.5). These changes lower the overall albedo of the system and thus continue and accelerate this positive feedback loop.

1.3 Sea Ice Mass Budget:

The waxing and waning of Arctic sea ice is a result of fluctuations between the thermodynamic (Term 2) and dynamic (Term 3) terms within the continuity or conservation of mass equation which is explained through equation 1 in figure 7. Equation 1 represents the change in sea ice thickness over time (term 1) but

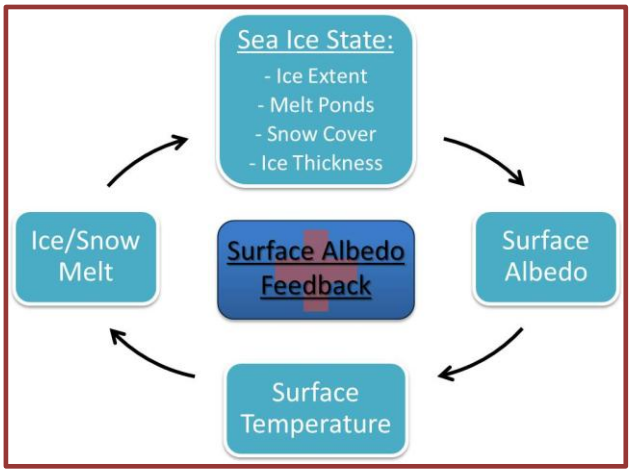

Figure 6 Flow chart describing the positive surface albedo feedback.

is also representative of ice volume continuity. The thermodynamic term considers interactions between radiative fluxes and the air and ocean temperatures that drive the melting and growth of sea ice annually. The dynamics term represents the movement of sea ice into and out of the Arctic basin. This term mostly applies to ice that is transported out of the Arctic basin to warmer waters and is subsequently melted. The focus of this study is on the thermodynamic term.

Sea ice growth occurs when the temperature of the ocean drops below -1.8 degrees Celcius, the freezing temperature of salt water. Conversely, the ice melts above this temperature. The growth and melt of the sea ice depends on other factors as well including the heat tranfer within, and at the top and bottom of the ice. Given that our focus is on the surface albedo feedback, further detail will be given to the thermodynamic term and more specifically the surface ice melt terms.

Continuity Equation for Ice Volume

$$\frac{\mathrm{d}\bar{h}}{\mathrm{d}t} = \Gamma_h - \nabla(\vec{u}h)$$

- Change in Ice Thickness (Ice Volume)

Figure 7 & Equation 1 The basic continuity equation for ice volume described by a thermodynamic and dynamic term.

$$F_{\text{net}}(T_o) = F_r(1-\alpha) - I_0 + F_L - \sigma T_o^4 + F_s + F_e + k\frac{\partial T}{\partial z}$$

Equation 2 governs the balanced energy flux at the ice surface.

Equation 2 governs the balanced energy flux at the ice surface. A positive net flux at the ice surface with temperature T_o, describes a melting ice surface and a negative net flux indicative of a non-melting ice surface. $F_r(1-\alpha)$ is the fraction of the downward shortwave radiation that is absorbed by the surface with F_r being the downward shortwave at the top of the atmosphere and alpha represents the surface albedo. I_o is the solar radiation that penetrates the top surface of the ice. F_L and σT^4 represent the incoming (downwelling) and outgoing long-wave radiation, respectively. F_s and F_l are the downward sensible and latent heat fluxes, respectively and the last term is the conductive flux from the sea ice ocean boundary towards the ice top surface. Here, we are most interested in the downwelling shortwave radiation and therefore examine the first term $F_r(1-\alpha)$ the most. [Bitz and Lipscomb 1999]. A summary of the terms used in this study is in figure 8.

1.4 Introduction Conclusion:

Arctic sea ice has a natural cycle of growth and melt with maximum ice extent realized in March and minimum in September; coinciding with the dark and light seasons. Therefore it is clear that the surface albedo feedback has the most profound effects during the summer months. Earlier melt season onset, which coincides during the time of peak shortwave solar radiation input, can amplify and accelerate the surface albedo feedback and is a key area of focus for this study.

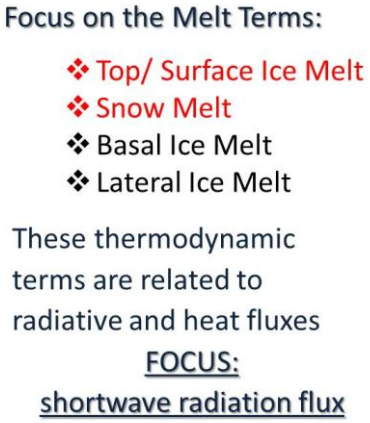

Figure 8 Summary of the thermodynamic melt terms with focus terms of this study in red. We then look to shortwave radiation fluxes in relation to these melt terms.

The present study focuses on the perennial sea ice of the Arctic Basin with an emphasis on examining changes in the surface albedo feedback between 3 temporally dissimilar model runs of NCAR's Community Climate System Model Version 4 (CCSM4): The pre-industrial (1850), 20th century, and 21st century model runs (integrations). The individual runs provide information on the state of Arctic sea ice and can be compared to assess change over time. Monthly output data from the model will allow for analysis of the general trends and will provide a framework for deeper analysis. This deeper analysis stems from the need to look beyond these monthly trends, realizing that sea ice changes on a smaller temporal scale and can be more accurately assessed through a daily data analysis. Therefore, to delve deeper into the cause and effect relationship of the surface albedo feedback, daily data were compiled by the model, providing an examination of variables not yet looked at in the modeling community.

This daily data helps to achieve better insight into which factors are dominant in driving and accelerating the surface albedo feedback and the resulting loss of sea ice. Specifically our project goals are as follows:

1. To assess the fundamental shifts and significance in long term trends in sea ice in relation to the surface albedo feedback. (seasonal, interannual, decadal).
2. To assess the effect of shortwave radiation fluxes on sea ice and how both together help drive the surface albedo feedback.
3. To assess whether or not these shifts or relationships vary over different regions of the Arctic.

These questions/goals listed above will be answered through analysis of output from the previously mentioned CCSM4.

2 Methods

To examine and decipher interactions between sea ice, atmospheric, oceanic, land, and other components, fully-coupled climate models are built, executed, and analyzed. These models use a system of differential equations to describe Earth processes and provide a comprehensive view of the climate system. In this study we use NCAR's newly released (April 2010) and completely coupled CCSM4, which has four main components and a coupler (figure 9)

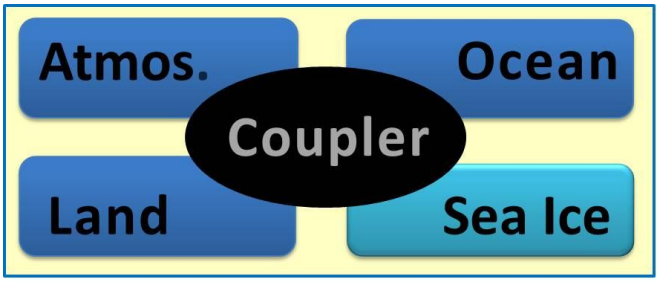

Figure 9 The CCSM4 is a completely coupled model with an atmospheric, oceanic, land, and sea ice components.

The CCSM4 has three model runs (figure 10) that provide the framework for this analysis. The 3 runs are the 1850 (pre-industrial) run, 20th century run or simulation, and the 21st century simulation. The 1850 (pre-industrial) control simulation was integrated using a constant greenhouse gas (GHG) concentration, an observation from the pre-industrial period. This simulation is run for over 1000 years in order for the system to reach equilibrium. This helps gauge the pre-industrial climate and natural variability within the system. The 20th century (1900-2005) run has prescribed GHG concentrations whose initial conditions are based on observations. The 21st century run (2005-2100) integrates a projection of future GHG concentrations, a future IPCC scenario. In this case, it is RCP 8_5.

Important to any model is knowing whether or not the model well simulates the actual climate system. Models are not, and should not be, expected to match observations exactly, due to the component of natural variability. To assess the robustness of the model, the 20th century run is analyzed in comparison to the limited observations that we have. The output is hoped to find trends similar, but not exactly the same (due to intrinsic variability), as the actual satellite observations. A good representation of the 20th century given by the model helps justify the predictions given by the 21st century run. In 2006, Arzel et al. found that from 1981 to 2000, "… the multimodel average sea ice extent agrees reasonably well with observations in both hemispheres despite the wide difference between models, which is less pronounced for the NH." Despite the wide intermodel scatter, the Community Climate System Model Version 3 (CCSM3), the predecessor to the CCSM4, is widely known for, "its good simulation of Arctic sea ice conditions and change over the late 20th and 21st century (Holland et al, 2006; Stroeve et al. 2007). Improvements in the CCSM4 lead to further accuracy. The main areas of physical improvements "…include new tracers, a new shortwave radiative transfer scheme, a melt pond scheme, and aerosol deposition, all applied to the snow and sea ice. (CCSM Website- HOW TO CITE THIS?)."These runs put out raw output data files which are stored on the National Center for Atmospheric Research's (NCAR) mass storage system. These data are not useful until a script is written which tells the supercomputer which data to extract from the mass storer and what to do with this data in order to create useful information. Linux was the operating platform used and emacs and vi editing programs were used to create these scripts which were written in both NCAR command language (NCL) and interface description language (IDL). Many thanks to Laura Landrum who wrote many of the basic scripts used to manipulate the model output. We altered these scripts to extract the variables that were most relevant to our study.

To gauge long term change that varies more than the natural variability, the 20th and 21st century runs are compared to the pre-industrial control simulation. For this, we used the model's monthly output data but will also be examining melt season characteristics through daily output data.

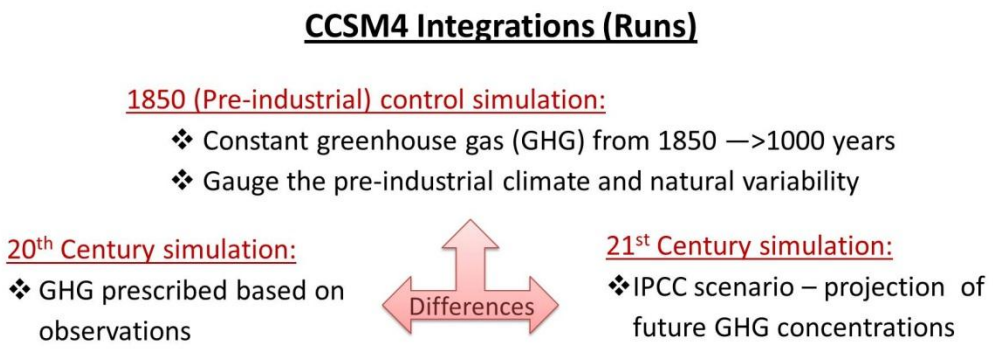

Figure 10 CCSM4 had three runs which were analyzed: the 1850 pre-industrial control simulation, the 20th century simulation and the 21st century simulation.

2.1 Monthly vs. Daily data:

From each of these three integrations stemmed two outputs for our purposes: monthly and daily data. The monthly data were used to diagnose the general and long term trends in Arctic sea ice state as well as the changes in the Arctic sea ice mass budget that describe these overall changes. While this data does provide a great diagnostic view of changes in the sea ice system, it fails at in depth analysis of sea ice melt timing, a critical component that influences the sea ice albedo feedback. To look at these specifics, daily output were examined, a rather newly examined metric in climate modeling. These daily data gave insight into melt season characteristics that exemplify the accelerating shifts seen in the monthly output data.

For both types of data, the most valuable information came from spatial maps and time series. The maps displayed the entire Arctic basin and showed the values of the desired term for the two time periods selected and more importantly the change between the two. In some cases, standard deviations and their differences between the time periods were also computed. Many different variables were examine for botht he daily and monthly data.

To pick an analysis time period, we first examined a time series of ice thickness from 1900 to 2100 which gave a diagnostic look at general long term sea ice changes (figure 11). The time series represents a combination of many variables that influence the overall ice mass budget. Given that daily data output was available up through 2055 at completion of this study, we selected the period from 1980 to 2050 for analysis given the large decreasing trend seen beginning in 1980. In 1980 the average basin ice thickness was 2.5 meters which dropped substantially to 1 meter by 2050. We also examined mass budget changes between the pre-industrial run and the 20th and 21st century runs, they are not the focus here (see appendix).

After selecting the time period 1980 to 2050 as the bounds of our study, we began analysis of the monthly data. Spatial plots looking at various metrics of general ice state and ice properties were created with 3 panels: 1981-2000 values, 2031-2050 values and difference between them. The difference plot provided background on the general trends.

Next, a similar spatial analysis was performed for the daily output data. This data

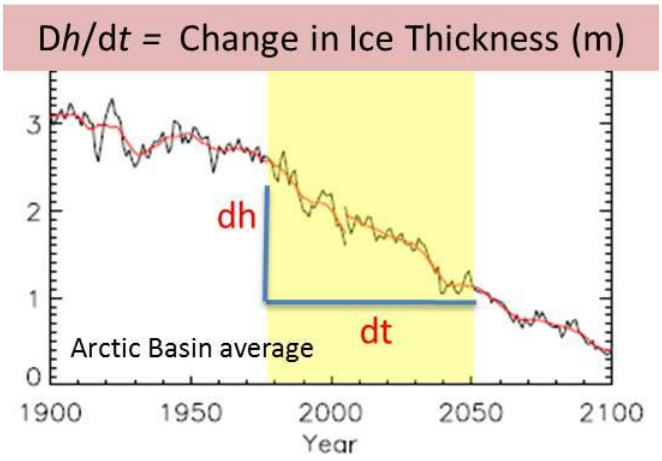

Figure 11 CCSM4 model output for ice thickness change between 1900 and 2100. The shaded region represents the study period and was selected due to the rapid decrease seen during this period.

Figure 12 Flow chart of the two temporally different data output and their uses within our methodology.

more in depth look at changes in melt season characteristics. Terms of key analysis included melt onset date, melt cessation (end) date, melt season duration, the total seasonal melt, and the maximum daily melt rate. After sorting through this data, the trends uncovered, were related to changes in shortwave radiation fluxes, giving insight into the effect of melt season changes and timing, and its relation to the surface albedo feedback. See figure 12 for an inclusive flow chart displaying these steps.

2.2 *Point selection & correlation value*s

From analysis of the spatial plots, 11 points were selected basin-wide on the basis of interesting or anomalous features. These points were clustered into 3 regions: Beaufort Sea, East Siberian Sea, and the Central Arctic (figure 13). For each of these points, decadal averaged time series were created for the entire suite of melt season characteristics described above. Additionally, similar decadal time series were created for ice concentration, downward shortwave radiation, absorbed shortwave radiation, and albedo. The latter three of these were created using output from the CCSM4

Figure 13 Map of points selected in the Arctic basin.

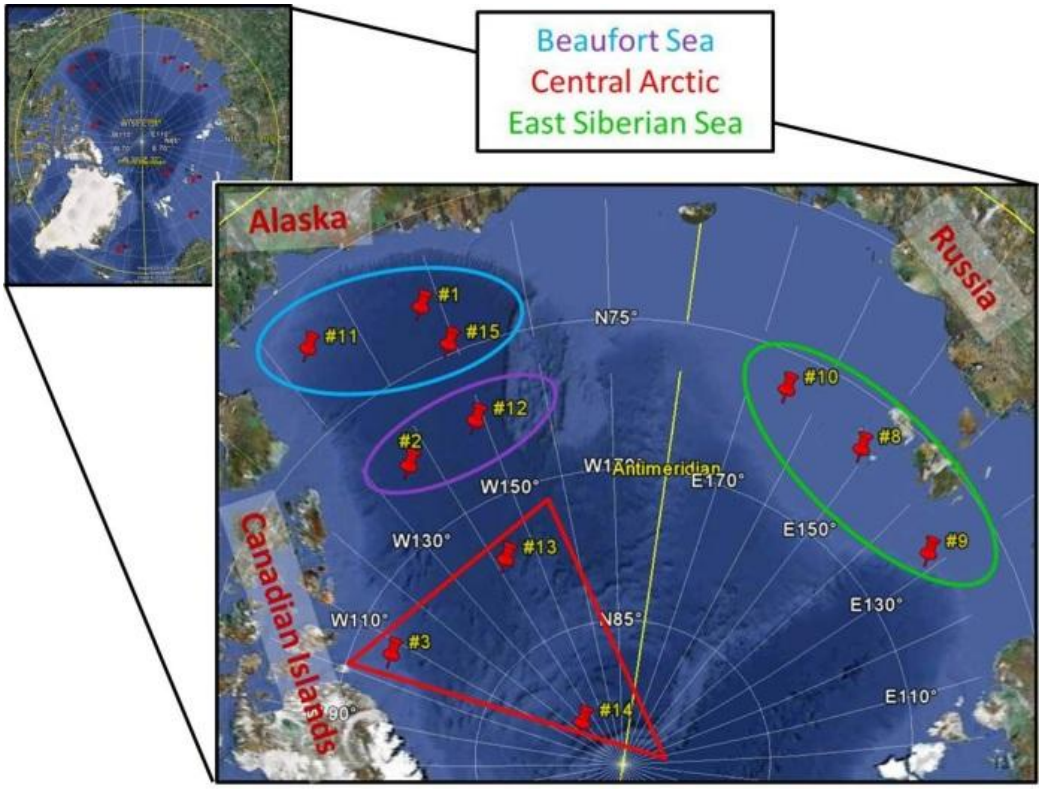

atmosphere model in addition to the CCSM4 sea ice model.

As a last point for analysis, correlation plots were created to see whether or not the results seen with these daily time series were significant. In particular we examined if there were strong correlation values (positive or negative) between absorbed shortwave radiation and melt season characteristics including melt onset, cessation dates, etc. Correlations values were ascertained by region.

3 Results and Discussion:

3.1 Long-term Change – Monthly Output Data

To supplement the basin averaged long term ice thickness change seen through the time series in figure 11, we created maps that display the spatial change in sea ice thickness and sea ice area concentration from across the Arctic basin. Figures 14 and 15 represent sea ice thickness and concentration changes from the first and last 20 years of the study period (1981-2000 ; 2031-2050). Values in these 20 year chunks are computed through the averaging of monthly model output data for the 20 years. The changes realized are substantial in both ice thickness and concentration change, but have opposite areas where there is greatest degree of change. For example, with the sea ice thickness change, areas in the central Arctic have the greatest change with some areas experiencing over 2 meters of loss, while the same area realizes a much smaller change in the ice concentration field. The opposite is also true with areas towards Alaska and Eurasia seeing smaller magnitudes of change and concurrently the highest decreases in ice concentration. While subtly noticeable at first, the rationale behind these changes are quite intuitive. Sea ice thickness change is highly dependent on the amount of sea ice that was there to begin with. The Central Arctic realizes the most change in thickness because there is simply more ice to melt, but experiences little concentration change because the area remains covered in ice year round. Coastal Alaska and Eurasia on the other hand, have seen a larger

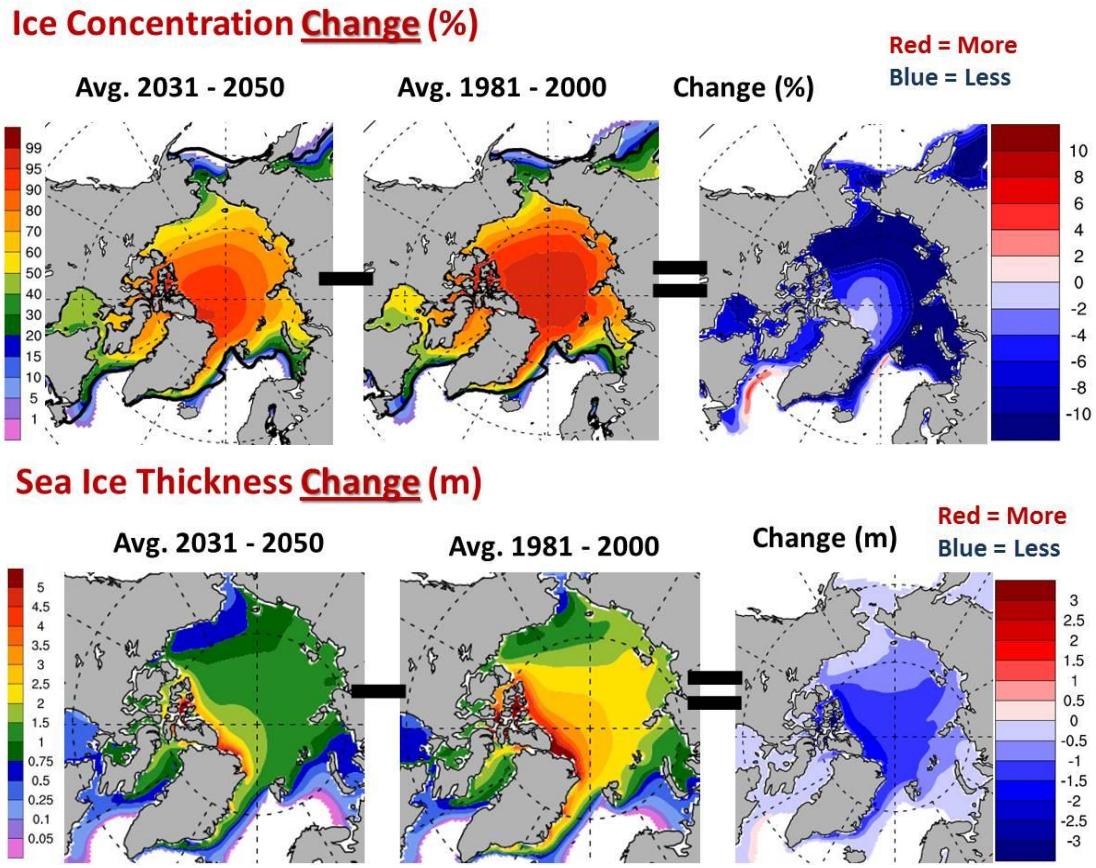

Figure 14 & 15 Spatial plots illustrating the changes in ice concentration (14) and ice thickness (15) between the period 1981-2000 and 2031-2050. Within both fields, substantial losses are seen across the entire basin. The black line in the middle panel illustrates the 10% satellite observed sea ice concentration for the same period. The location of line in relation to the model output 10% contour explains that the CCSM4 well represents the change seen in the real Arctic system.

concentration change as seasonally ice free conditions ensue, but see lower magnitudes of ice thickness change because there is simply not as much ice to melt in these regions.

The data depicted in figures 14 and 15 are derived from the model's monthly output data. As stated earlier, it is a prime goal of any climate model to similarly reproduce observations. We are confident that the CCSM4 does well represent the actual system. By looking at the plotting of the average 1981-2000 satellite 10% ice concentration contour represented by the thick black line in the middle panel of figure 14, it follows the blues which are around that percent concentration range. This soundness of model output versus observations provided confidence that trends seen in the forthcoming daily output data have real implications in relation to the real Earth system.

3.2 Changes in Melt Season Characteristics – Daily Output

For the daily output, melt season characteristics were described by a series of threshold with windows. For both the top ice and snow melt the threshold for determining the melt start and cessation date of melt was when melt dropped above/below 0.02 cm per day for a period of 5 days. This threshold was held for the entire study period. The soundness of these thresholds was examined through the regional analysis time series detailed in the next section.

The output from the model provided great insight into the changing state of Arctic sea ice and gives rise to other implications in need of discussion. Looking to figures 16 and 17, we see the spatial maps of this daily change. These maps exhibit changes in melt onset and end date for each of the two periods, along with the change between them. This is representative of the melt season length change. At first, it was interesting to note the difference between the highly spatial dependence on melt end date versus the onset

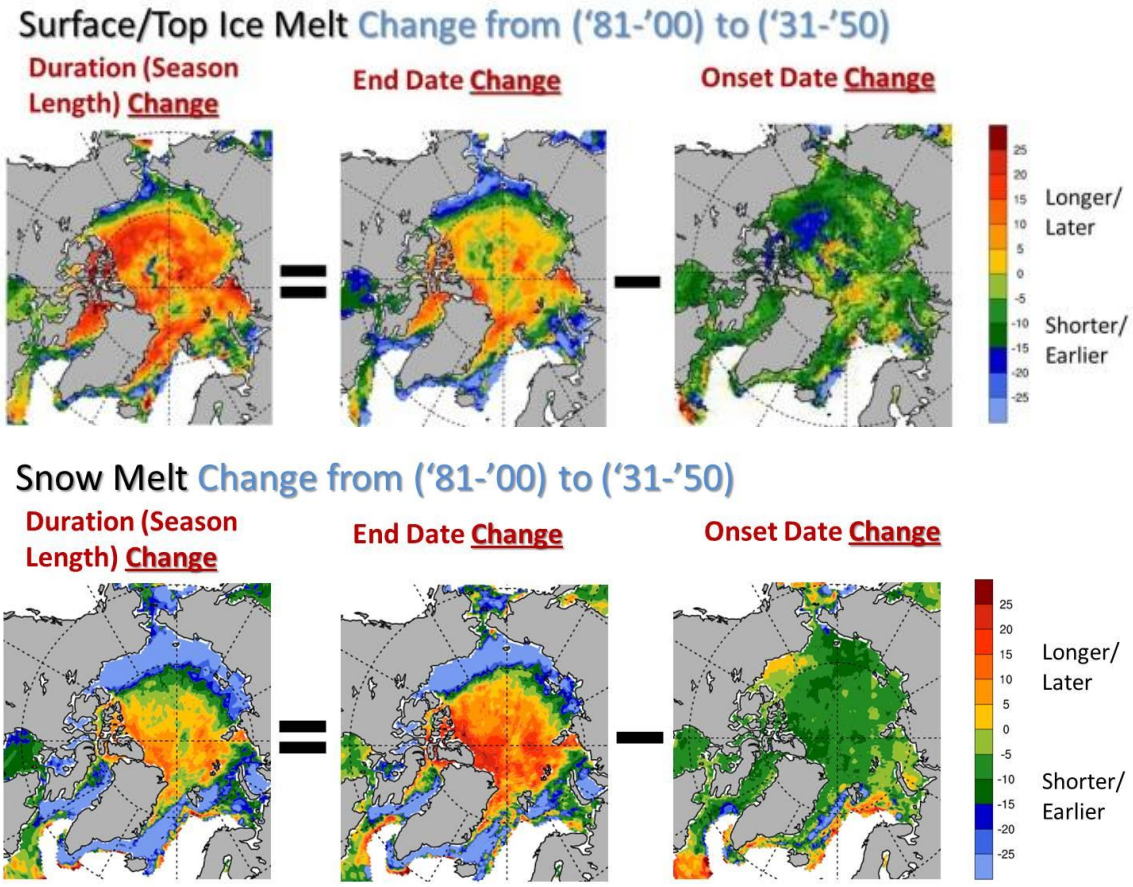

Figure 16 & 17
These spatial maps show the changes in season duration, end date, and onset date between the period 1981-2000 and 2031-2050. Figure 16 (17) illustrates surface/top ice melt (snow melt). Differences over time in the duration and end date metrics are rather intuitive. But very interesting to note is the uniform shift towards earlier melt onset dates seen basinwide.

date change which saw nearly uniform changes basin-wide. Changes to a longer melt season and later dates are represented in the yellows and reds while changes to a shorter melt season and earlier dates are displayed in the greens and blues.

Changes in end date require explanations similar to those in the monthly data. Due to the increased melting that is indicated above, central Arctic areas are melting later because there is more ice to melt. Ice in areas close to the Alaskan and Eurasian shore are melting through seasonally leading to an earlier end date.

More important and intriguing to this study and to the larger study of Arctic sea ice in the climate system is the nearly uniform change towards earlier melt onset dates seen across the entire Arctic basin. These earlier dates coincide with the seasonal maxima of incoming solar radiation, which helps to clarify factors behind why models are predicting these large downward trends in Arctic sea ice. Examination of the combined effect of earlier onset dates and the seasonal maximum in solar radiation are of great importance and are discussed later. First though, a regional analysis of these melt season characteristics is performed.

3.3 Regional trends in melt season characteristics:

The regional analysis gives a numerical and graphical view of the changing Arctic sea ice state and also allows for an analysis by decade, giving a higher temporal resolution of melt season changes. Look back to figure 13 for the map of the 11 points that were selected for this analysis. Notice also that they are classified into three regions, one of which has two sub-regions. The blue and purple circled areas are the outer and inner Beaufort Sea regions, respectively. The points in the red triangle are considered the Central Arctic and the three points circled in green are in the East Siberian Sea region.

Plots representing the change in days for each of the melt season metrics by point and region were created. figures 18a,b,c show the top ice onset date, end date, and duration change in days through decadal averages from 1980 – 2040.

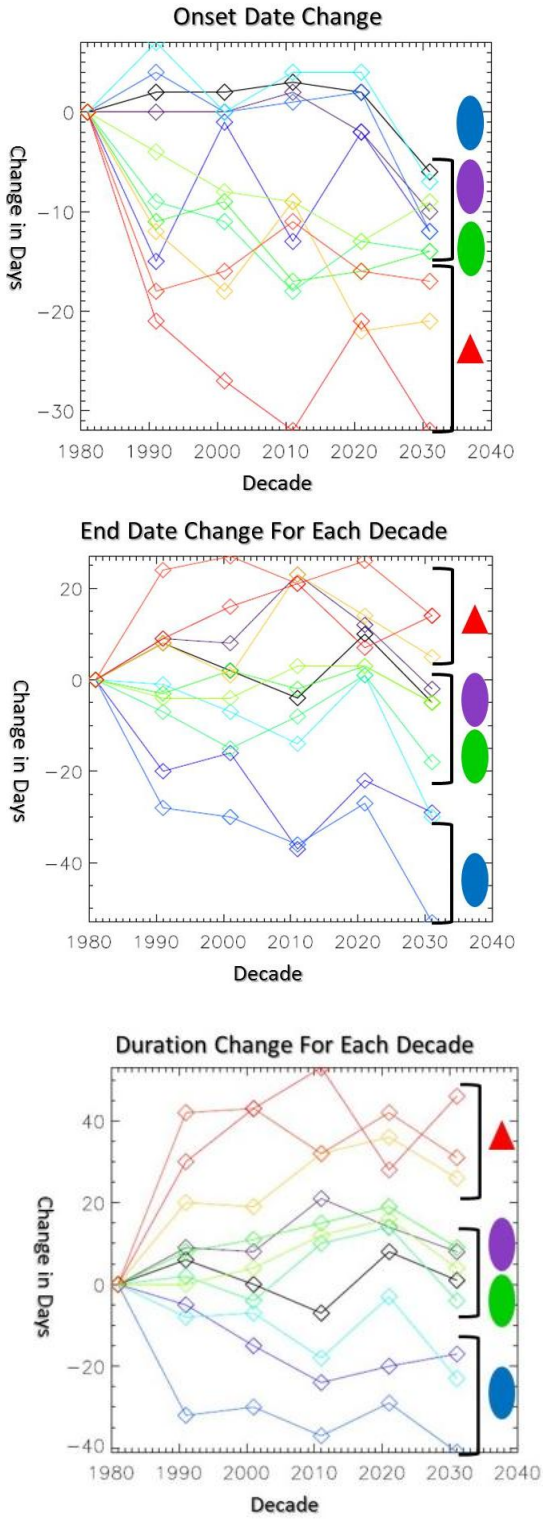

Figure 18(a,b,c) are time series displaying the changes in melt season characteristics by decade for each of the 11 points. Regional trends are noted and are comparable to the spatial plots. Note that on the onset date change plot (18a) nearly all points see an early onset trend. The triangle and oval symbols represent the regions described in Figure 13.

The onset date change (figure 18a) solidifies the findings above showing that by 2031-2040, all points and regions are experiencing melt from a week to as much as a month earlier than in the decade from 1981-1990. The central Arctic sees the largest change because the area had only recently experienced major seasonal melting. Coastal Beaufort Sea saw the least change because it had already seen large melting. Interesting to note though is the large drop seen by the 2031-2040 decade.

The changes in end date and season duration (figures 18,b,c) are what we would expect; Central Arctic areas see the latest melt cessation dates and largest duration change while areas closest to the coast in the Beaufort sea see the opposite. An interesting trend to note is in the end date change which seems to reveal a drop off to earlier end days in the purple, green and blue regions during the last decade of analysis. Perhaps this and the large drop seen in the onset date represents an abrupt change during this period; This type of analysis is not within the scope of this paper.

3.4 Daily time series by decade – selected points

For each of the 11 points, a time series was created showing decadal averages of melt magnitudes per day along with symbols indicating melt onset and cessation dates (diamonds) and the day of maximum melt magnitude (asterisks). The placing of these symbols depends on the thresholds and window set above. Also, to make the time series smoother, a 3-day running average was implemented. The x-axis represents the day of the year in Julian calendar days and extends between day 100 and 300, days in the boreal summer. The y-axis represents the amount of melt in cm/day (Note the difference in max y-axis scales between the two points). To gauge the total melt, you can roughly estimate the area under each curve (take integral).

Selected and shown here are the time series of top ice melt and snow melt for point #2 and point #14. These time series have lines indicating the daily output decadal averages for the entire study period from 1980 to 2050. Points #2 (Inner Beaufort Sea) and #14 (Central Arctic-near North Pole) were selected on the basis of their location and the different ice conditions that are experienced at each.

Trends towards earlier melt onset as well as higher overall seasonal melt are obvious by glancing at the ice top melt time series (figure 19a – point #2 , figure 20a – point #14). For the decade 1981-1990, little melt is realized with point 14 experiencing very little melt (black line). As time progresses, this changes with 2 large shifts realized in the decades 2001-2010 and 2041-2050. The shift in 2001-2010 is highly evident in point 2 as well is the trend towards earlier onset, max melt, and end dates as would be indicated by a line connecting each. At point 14, the take away message is the significant increase in total melt experienced during 2041-2050. At both locations, it is concretely clear that magnitudes of top ice melt are increasing drastically as well as the timing which is indicated by the leftward shifting peak.

Similar trends are seen with snow melt, but are more chaotic as expected. Snow melt is a function of how much snow there is which relies heavily on the weather and thus the atmosphere component of the model. Even still though, general trends towards earlier melt onset dates as well as earlier peak dates are evident (figures 19b, 20b).

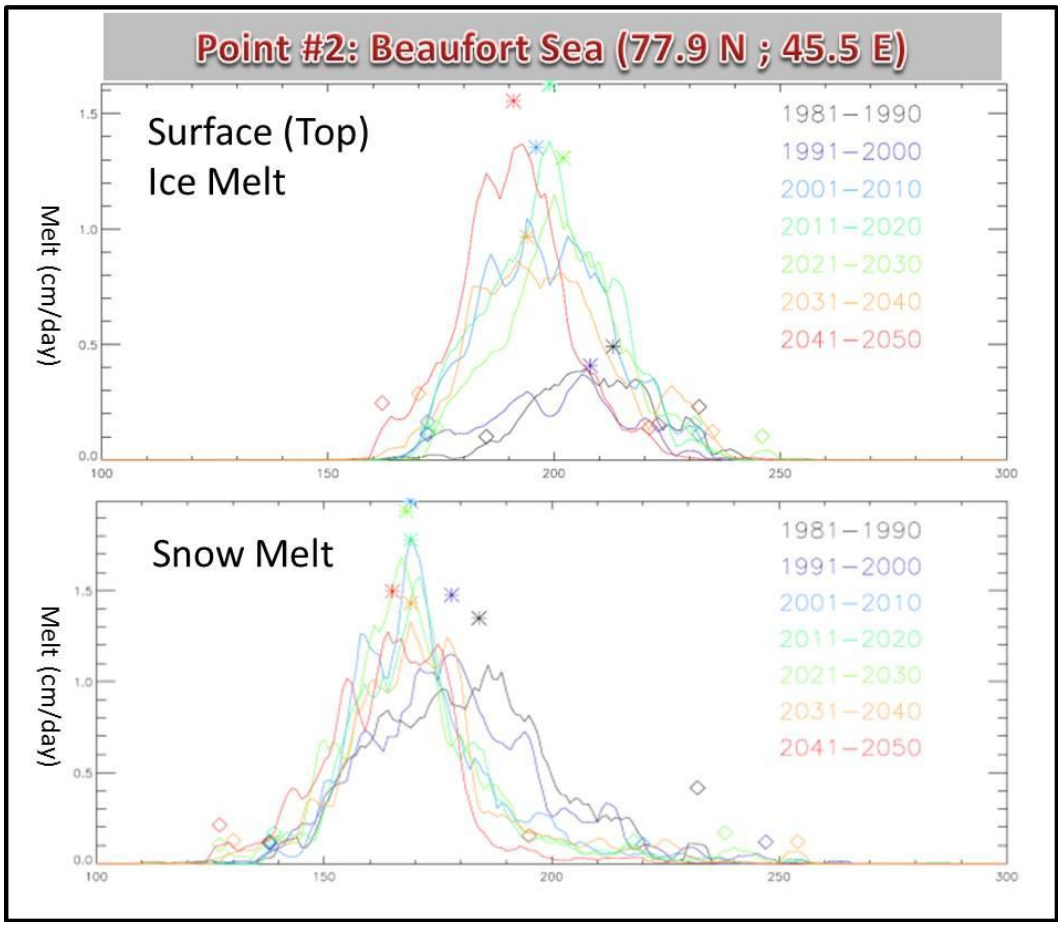

Figure 19(a,b,) are time series of daily melt (a=top melt; b=snow melt) at Point #2. Illustrated are curves for each decade. Diamonds indicate onset and end dates and the asterisk indicates the day of max melt. Shifts towards earlier melt date and higher seasonal melt are distinctly visible.

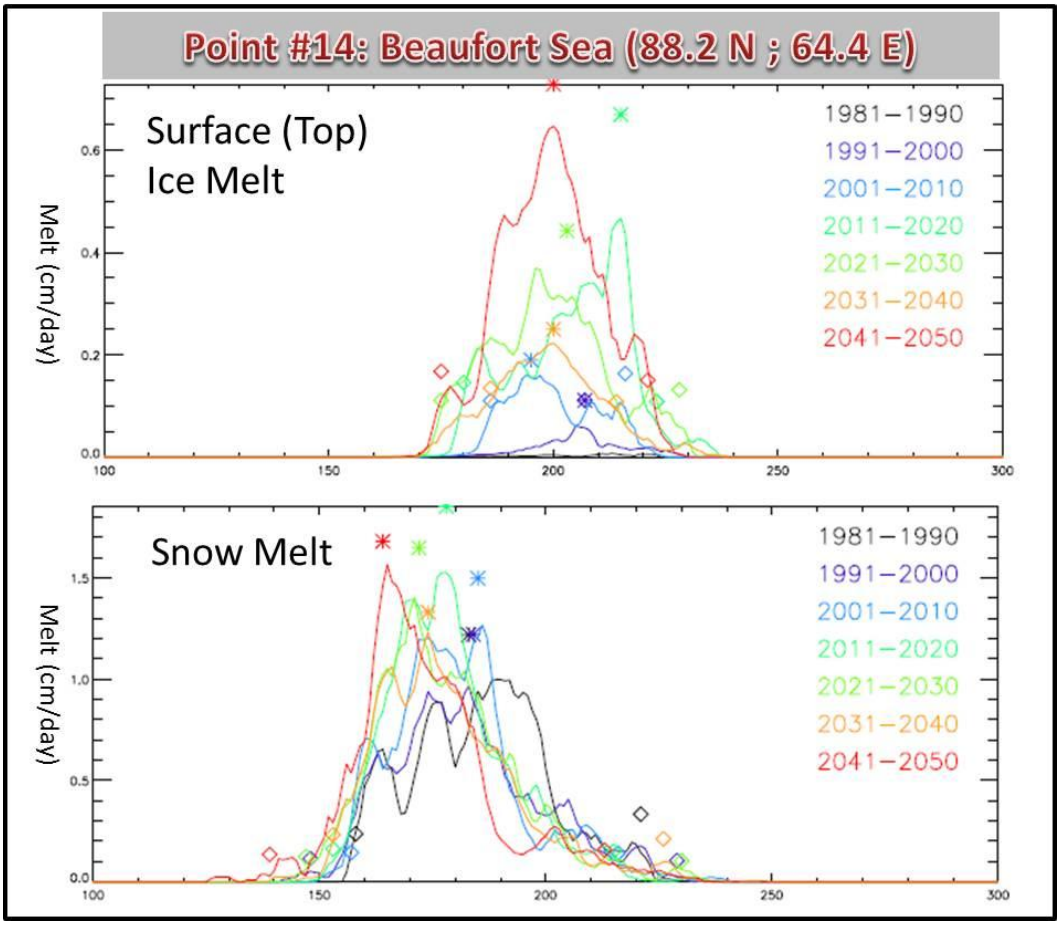

Figure 20 (a,b,) are time series of daily melt (a=top melt; b=snow melt) at Point #14. Illustrated are curves for each decade. Diamonds indicate onset and end dates and the asterisk indicates the day of max melt. Shifts towards earlier melt date and higher seasonal melt are distinctly visible.

3.5 Seasonal Shifts and Shortwave Fluxes

Already significant in its own, the basin wide trend towards earlier melt onset dates has further implications given the coinciding maximum solar input seen concurrently. It is around these times, the summer solstice, when the sun is highest in these polar regions and therefore the downwelling solar radiation is the highest. Figure 21 shows the monthly-averaged downward shortwave radiation for the study period at point 2. Visible is the seasonal cycle with no solar radiation during the winter months and a maximum in the months of May and June, when the snow and ice start significantly melting in the Arctic. In the figure focus on the dotted lines that run from the points in June, when insolation peaks at 268 W/m^2 versus September when insolation is at 38 W/m^2 and also when Arctic sea ice reaches its minimum extent. Intuitively most would think that since there is most open ocean during the months of August and September, that the surface albedo feedback would be most enhanced and pronounced during these months. This is not the case due to the low amounts of insolation. In fact, during the months of May and June, when a large portion/majority of the basin is still ice covered, is when the enhancement and acceleration of the surface albedo feedback is likely the largest. Given the large solar input during these months, even a small change in the average albedo due to earlier melting (figure 22), could invoke large changes on the system and reinforce an enhanced feedback for the remainder of the melt season. This is equally visible in figure 23 which displays the amount of absorbed shortwave radiation at the same point. The increased absorption in the 2041-2050 decade is deeply correlated with the expansive decrease in ice concentration realized by 2050. (figure24). Notice that in the months of May and June, the changes in ice concentration are not noticeable. Even though the ice is still present during these months, lower albedos (figure 22) are realized on the ice through melt ponds and as a consequence, more shortwave radiation is absorbed (figure 24). These slightly lower albedos (a 0.1 decrease), and increased shortwave absorption, clearly explain the

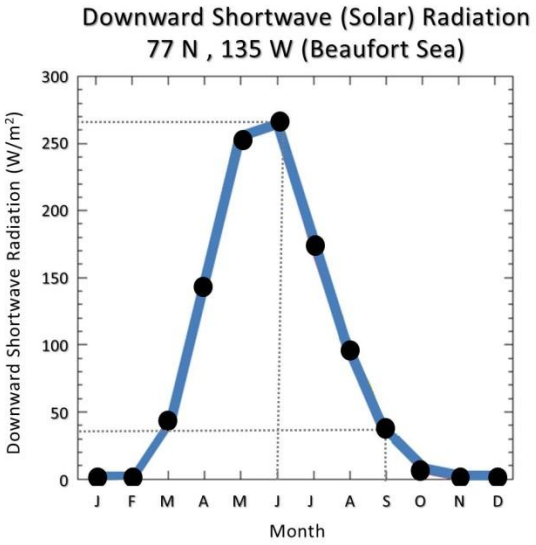

Figure 21 Average monthly incoming solar radiation for one point in the Arctic. Note the vast difference in solar radiation flux between May/June and September.

substantial drop off in ice concentration seen by the middle of the 21st Century, through the surface albedo feedback.

3.6 Melt Season Characteristics and Shortwave Absorption Correlations

Correlation values were computed between melt onset and end dates and the amounts of absorbed shortwave radiation in the system. These correlation values are insightful in that they help discover whether or not the amount of shortwave absorption is related to changing melt onset and cessation dates. Positive correlation values indicate that later dates are

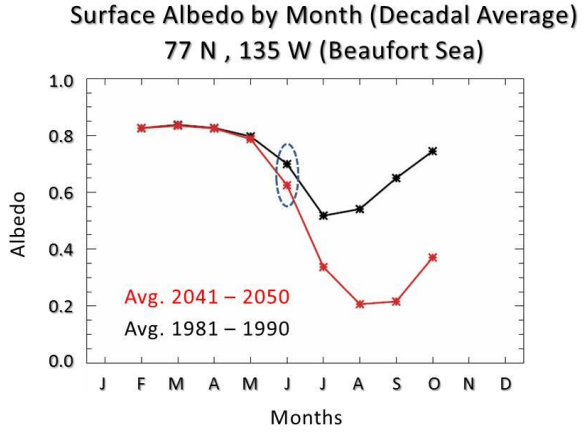

Figure 22 Surface albedo change by month from the 1980s to 2040s. Large changes in albedo in the month of June are likely the cause of the significant drop of seen in August and September.

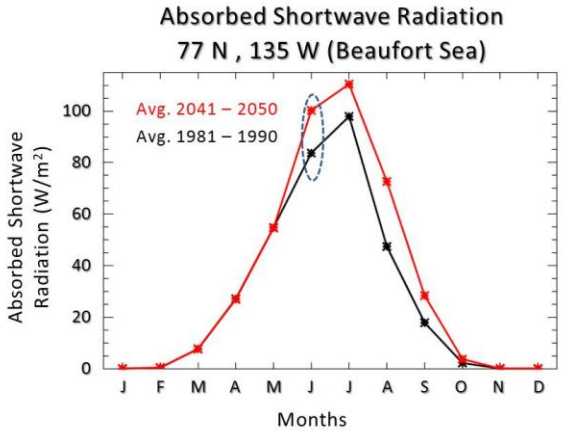

Figure 23 Shortwave Absorption increase by 2041-2050 due to lower albedos and thus larger areas of open ocean.

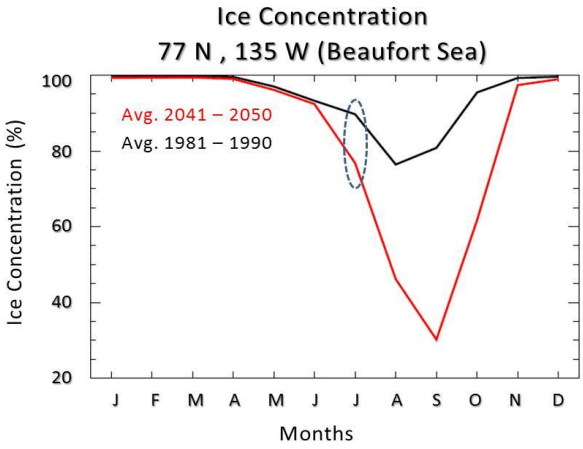

Figure 24 The decrease in average monthly ice concentration by 2050 is clear here. The largest changes are seen beginning in July. Large scale effects of the decreased albedo and increased shortwave absorption are seen by July.

associated with more absorbed shortwave. Negative correlation values indicate that earlier onset/end dates are coupled with increased shortwave absorption.

The correlation value tests revealed that there were relatively strong negative correlations in all regions for melt onset dates; both for surface ice melt (figure 25) and snow melt (figure26). Therefore we are confident that the change in melt onset dates, even the subtle 1 or 2 week change, has substantial consequences in regards to increased shortwave radiation absorption. This confirms that this earlier shift is likely accelerating the surface albedo feedback through the addition of heat to the system (Refer back to figure 6). As suspected, weaker correlations are seen with melt end dates.

Sfc/Top Ice Melt	Onset	End
Beaufort Sea	-0.54	-0.38
Central Arctic	-0.48	-0.14
East Siberian Sea	-0.79	-0.32

Snow Melt	Onset	End
Beaufort Sea	-0.53	-0.42
Central Arctic	-0.46	0.03
East Siberian Sea	-0.58	-0.45

Figure 25,26 Correlation values by region between onset dates and absorbed shortwave for both surface/top ice melt and snow melt. Strong correlations are seen between earlier onset date and increased shortwave. Weak correlations are seen in regards to melt cessation dates.

4 Summary and Conclusion

Over the past 30 years, satellite observations have indicated significant decreases in Arctic Sea Ice extent and volume. NCAR's Community Climate Systems Model Version 4 (CCSM4) closely documents this change and therefore gives confidence in its projected output for the future . The model also confirms that anthropogenic inputs are indeed a leading cause of recent ice state change . Monthly model output data indicate substantial decreases in ice concentration and ice extent by the end of our study period (1980 – 2050). These decreases in Arctic sea ice can be largely attributed to changes in the surface energy budget through the surface albedo feedback.

The surface albedo feedback is a positive feedback loop which describes the cycle between decreased albedo, increased temperatures, and increased ice melting. It is a viscous cycle that is projected to continue to amplify and accelerate. A fundamental reason behind this acceleration is realized shifts in melt season characteristics. Changes in melt cessation dates and melt season durations were spatially dependent, and are not out of the ordinary. Interesting to note though were the changes in melt onset date. Melt onset date changes from 1980 to 2050 were uniform and revealed earlier onset dates basin wide.

There are substantial implications when coupling this trend towards earlier melt onset date and the timing of maximum solar input. Melt in the Arctic basin occurs during the months of May and June, coincidentally when the sun is highest in the sky. As a result, small changes in sea ice albedos from earlier melt onset dates have the potential to cause drastic changes in sea ice during the remainder of the season. The later decades of our analysis strongly display ILLUSRATE these changes. Strong negative correlation values confirm that earlier onset dates are highly related to increased shortwave radiation absorption.

The surface albedo feedback is one of the most influential mechanisms in the changing state of the Arctic sea ice pack. Like most models, the CCSM4 predicts that the long-term future of sea ice extent and volume is trending down. Here, we've looked for reasons behind these changes through analysis of melt season characteristics. While many other factors play a role in sea ice changes, the surface albedo feedback plays a significant role in the overall Arctic and global climate system. This positive feedback will have increased significance in the coming years as earlier melt onset dates coupled with peak solar input lead to an accelerated surface albedo feedback.

Acknowledgements I would like to thank my mentors Marika Holland, David Bailey, Cindy Worster, and Alexandra Jahn for their assistance throughout the summer. Also many thanks to the SOARS staff Rajul Pandya, Rebecca Haacker-Santos, and Moira Kennedy for the opportunities and support they provide throughout the summer.

References

Arzel, Oliver, Tierry Fichefet, Hugues Goosse, 2006: Sea ice evolution over the 20th and 21st centuries as simulated by current AOGCMs, *Ocean Modelling*, **12.3/4**, 401-415, doi:10.1016/j.ocemod.2005.08.00

Bitz, C. M., William H. Lipscomb, 1999: An energy-conserving thermodynamics model of sea ice, *Journal of Geophysical Research* **104**, C7, 15,669 -15,677, doi:10.1007/s00382-008-0493-4

Bony, Sandrine, and Coauthors, 2006: How Well Do We Understand and Evaluate Climate Change Feedback Processes?. *J.Climate*, **19**, 3445–3482.

Holland, M. M., J. Finnis, A. P. Barrett, and M. C. Serreze (2007), Projected changes in Arctic Ocean freshwater budgets, *J.Geophys. Res.*, **112**, G04S55, doi:10.1029/2006JG000354.

Holland, Marika M., 2010: Arctic Sea Ice and the Potential for Abrupt Loss, *Geophysical Monograph Series* doi:10.1029/2008GM000787

Holland, Marika M., C. Bitz, L. Tremblay, D. Bailey, 2008: The Role of Natural Versus Forced Change in Future Rapid Summer Arctic Ice Loss, *Journal of Geophysical Research*, doi:10.1029/180GM10

Holland, M. M., C. M. Bitz, and B. Tremblay, 2006b: Future abrupt reductions in the summer Arctic sea ice, *Geophys. Res. Lett.*, **33**, L23503, doi:10.1029/2006GL028024.

Holland, M.M. and C.M. Bitz, 2003: Polar amplification of climate change in coupled models, *Clim. Dyn*, **21**,221-232, doi:00382-003-0332-6.

Manabe, S. and Stouffer, R. J., 1980: Sensitivity of a global climate model to an increase of CO2 in the atmosphere, *J. Geophys. Res.*, **85(C10)**, 5529–5554.

Menne, M.J., J. Kenedy, 2008: Global surface temperatures in 2008 [in "State of the Climate in 2008"], *Bull. Amer. Meteor. Soc.,* **90** (8) S17 – S18.

Serreze, Mark, M. M. Holland, J. Stroeve, 2007: Perspectives on the Arctic's Shrinking Sea-Ice Cover *Science* **315** doi:10.1126/science.1139426

Serreze, Mark, C., A Barrett, J. Stroeve, D. Kindig, M. Holland, 2009: The emergence of surface-based Arctic amplification, *The Cryosphere*, **3**, 11-19.

Stroeve, J., M. M. Holland, W. Meier, T. Scambos, M. Serreze, 2007: Arctic sea ice decline: Faster than forecast, *Geophys. Res. Lett.*, **34**, L09501, doi: 10.1029/2007GL029703, 2007

Rind, D., R. Healy, C. Parkinson, and D. Martinson, 1995: The role of sea ice in 2 x CO2 climate model sensitivity. Part I: The total role influence of sea ice thickness and extent. *J. Climate,* **8,** 449–463.

Vavrus, Steve, 2004: The Impact of Cloud Feedbacks on Arctic Climate under Greenhouse Forcing*. *J. Climate*, **17**, 603–615.